Laser wakefield electron accelerator: possible use for radioisotope production

Nilson Dias Vieira Junior
IPEN/CNEN
São Paulo/SP, Brazil
nilsondiasvieirajr@gmail.com

Edison Puig Maldonado
Instituto Tecnológico de Aeronáutica
São José dos Campos/SP, Brazil
puig@ita.br

Alexandre Bonatto
UFCSPA
Porto Alegre/RS, Brazil
abonatto@ufcspa.edu.br

Roger Pizzato Nunes
UFRGS
Porto Alegre/RS, Brazil
roger.pizzato@ufrgs.br

Sudeep Banerjee
Arizona State University
Tempe/AZ, USA
sudeep.banerjee@asu.edu

Frederico Antonio Genezini
IPEN/CNEN
São Paulo/SP, Brazil
fredzini@gmail.com

Mauricio Moralles
IPEN/CNEN
São Paulo/SP, Brazil
moralles@ipen.br

Armando V. F. Zuffi
IPEN/CNEN
São Paulo/SP, Brazil
armandozuffi@gmail.com

Ricardo Elgul Samad
IPEN/CNEN
São Paulo/SP, Brazil
resamad@gmail.com

2021 SBFoton International Optics and Photonics Conference (SBFoton IOPC) | 978-1-6654-1948-2/21/$31.00 ©2021 IEEE | DOI: 10.1109/SBFOTONIOPC50774.2021.9461976

***Abstract*—Electron beams generated by laser wakefield acceleration can induce a photoneutron reaction to convert ^{100}Mo into ^{99}Mo. Multi-pC, several-MeV electron beams, obtained from particle-in-cell simulations, could generate bremsstrahlung gamma photons within the absorption region of the photonuclear reaction. The efficiency of this process is estimated for a laser accelerator operating at kHz repetition rate in the self-modulated regime. The electron beam kinetic energy must be improved to 40MeV. To meet the typical consumption of ^{99}Mo per patient within its decay timescale, this efficiency must be increased by three orders of magnitude.**

Keywords—Laser wakefield, photoneutron reaction, radioisotope, nuclear medicine.

I. INTRODUCTION

Laser wakefield acceleration (LWFA) has been a rapidly growing field since the seminal paper by Tajima and Dawson [1] in 1979 and is becoming a mature field capable of taking part in many new applications, competing and complementing conventional radio-frequency based accelerators [2-4]. Most of this progress is due to advances in solid state lasers that brought compactness and reliability, allied with exceptional optical properties like producing high peak powers (a combination of high energy pulses with ultrashort pulses) that, in combination with nonlinear phenomena and light manipulation, like chirped pulse amplification (CPA) [5] and self-phase modulation [6, 7], resulted in the achievement of a few PW peak power systems, enabling the generation of the highest electric and magnetic fields ever produced in laboratories [8] [9].

One of the most exciting results of the wakefield particle acceleration is the downsizing resulting from the plasma electrical fields produced by laser pulses in gases and the short pulse duration of the electron bunches. This LWFA produced electron beams with kinetic energies up to several GeV [10] within centimeter-long propagation distances. The main limitation for practical LWFA applications is the laser average power, which is low for systems operating at very high intensities. Such limitation is being surpassed by a combination of distributed gain (and distributed thermal problems) in optical fibers, in combination with spectral broadening and chirp compression, leading to pulses with few fs duration [11, 12] and high repetition rates. In the continuous wave mode, average powers of hundreds of kW are already commercial [13].

The main idea of this work is to use the LFWA technique to generate electron beams with kinetic energy in the range or above dozens of MeV, capable of generating gamma rays by bremsstrahlung with several MeV energy, similar to the idea used with Cu and Au [14, 15]. These gamma ray photons will be used to induce the ^{100}Mo (γ, n) ^{99}Mo photonuclear reaction in enriched ^{100}Mo targets, and as a final product, deliver either the nucleus ^{99}Mo, which has a half-life of 66 h, or its metastable daughter ^{99m}Tc. The latter is the most used radionuclide in nuclear medicine for diagnostic of coronary and cancer diseases [16, 17], with a consumption that grows as these diseases are aggravated with population aging.

The estimated cost of a gram of ^{99}Mo is of several hundreds of million dollars, what makes feasible the construction of nuclear research reactors to produce ^{99}Mo as a fission product. However, developing a lower-cost, environmentally safer ^{99}Mo production method is imperative to supply the ever-growing demand for it.

Nowadays, there are many proposals for using electron accelerators to induce ^{99}Mo by nuclear reactions, despite the known state-of-the-art less effective production path [18-20], because the absorption cross sections for the ^{100}Mo for photoneutron is high (1.5×10^{-25} cm^2) [21] due to the giant resonance around 14.5 MeV [21]. The main problem is the specific activity, which is reduced in natural Molybdenum, and besides, the isotope separation methods are difficult to implement in the time scale of the nuclei decay, leading to the extraction of the ^{99m}Tc that presents a short lifetime of ~6h [22]. In spite of these disadvantages, a strong effort in this direction is being made across the world, because of the huge medical need for this isotope and the aging of the producing nuclear reactors [23]. This work considers the use of electron LWFA instead of RF accelerators for demonstrating the feasibility of ^{99}Mo or ^{99m}Tc production by photoneutron reaction in its fundamental aspects only. Technologically, these two techniques are not comparable, because one is already mature (RF) and LFWA is just starting. Additionally,

This work was supported by FAPESP.

978-0-7381-2418-6/21/$31.00 ©2021 IEEE

the average consumption of ^{99}Mo per patient [24] is ~20 ng, so individual doses are within a small-scale production, compatible with the present study. There is an uncertainty in this quantity, and by local standards, can vary by a factor 2, due to the decay time and the usual procedures in the medical clinics. To produce the annually needed ^{99}Mo by this process, many high-repetition lasers would be needed in a new distributed logistic, which can be achieved more easily by using the Self-Modulated Laser Wake Field Acceleration (SM-LWFA) regime, since the laser requirements are more flexible (pulse duration, energy, and peak powers), making it easier to combine them all in simple systems with an expectation of lower costs and easier maintenance.

This work is part of an ongoing collaboration with the Extreme Light Laboratory (ELL) at the University of Nebraska-Lincoln (UNL) and will be supported by the LaserNetUS cycle 3. The primary goal is to attain electron beams with more than 10 MeV energy generated by SM-LWFA, from a few TW laser pulses. In addition, many facilities can now operate in the SM-LWFA at ~kHz repetition rates. Assumptions on the ^{99}Mo activity production need will be presented.

II. Operation conditions of the accelerator: LWFA and SM-LWFA regimes

The idea of LWFA was boosted by experimental demonstration of collimated and several MeV energy electron beams, in the resonant regime [25-30]. The resonant condition can be stated as:

$$c\,\Delta t = \lambda_p/2 = w_0, \tag{1}$$

where c is the speed of the light, Δt is the optical pulse duration and w_0 is the laser pulse beam waist. This condition is a compromise between the transverse and longitudinal electrical fields that create a longitudinal acceleration field (wakefield) in the presence of the transverse optical field in a rarefied medium (gas). To match the requirements between pulse energy and duration in the usual LWFA systems, peak powers of more than 100 TW are applied, generating electrical fields that will match the plasma field at w_0. This resonance requires relatively long plasma wavelengths (and low plasma densities). Nowadays, GeV electrons are obtained using the same concept and increasing the acceleration length [31]. The physics of this regime is now well established and can be found in excellent reviews [28, 29, 31]. The fundamental quantity of this regime is the plasma frequency, ω_p, which depends on the electron density according to:

$$\omega_p = [(n_e\, e^2)/(m_e\, \varepsilon_0)]^{1/2}, \tag{2}$$

where e is the electron charge, ε_0 is the vacuum permittivity, n_e is the electron density and m_e is the electron mass. The critical plasma density, n_c, is given by:

$$n_c = \varepsilon_0\, m_e\, (\omega/e)^2. \tag{3}$$

For Ti:sapphire lasers (λ=0.8 μm, $\omega = 2.35\times10^{15}$ rad/s), the critical density is 1.7×10^{21} e$^-$/cm^3.

Considering that the plasma supports a wakefield pushed by the optical pulse, which moves with the group velocity of light in the medium (approaching c) the plasma wavelength λ_p can be written as:

$$\lambda_p\,(\mu\text{m}) \approx 3.3\times10^{10}\times[n_e\,(\text{cm}^{-3})]^{-1/2}. \tag{4}$$

The resonant condition scales with the pulse duration in the longitudinal direction, and with its area in the transverse direction, according to Eq. (1), therefore the pulse energy scales $\propto w_0^3 \propto \Delta t^3$ and $\propto$ to λ^3 (regime named λ^3), when the pulse duration is in the order of the period of the carrier frequency. The main advantage of using few cycle pulses is that the decrease in pulse duration by one order of magnitude causes the decrease of 3 orders of magnitude in the required energy to match the resonant condition [32], lowering the required power from PW to TW. With the advance in lasers systems, decreasing the pulse duration to a few cycles allows the use of TW peak powers with few mJ pulse energies, allowing the operation at kHz repetition rates in the resonant LWFA regime.

Recently, two different groups [29, 30] have achieved LWFA in the λ^3 regime with few cycle pulses (few fs). These spectrally broad and short pulses demand special care to reach the gas targets. There are few systems operating with these features nowadays. Usually, the pulses are longer, in the range of tens of fs, and the power is in the 100 TW range. In these two experiments, the total detected electron beam charge was in the range from 2.5 to 10 pC, and the electron kinetic energy in the 15 MeV region. Among the different injection mechanisms, the nonlinear relativistic self-focusing is one that focuses the beam and increases the intensity in a nonlinear way breaking the response of the plasma (wave-breaking). The condition for this is given by a power law that depends on the plasma density, expressed as the critical Power P_c:

$$P_c = 17.4\ \text{GW} \times\ (n_c/n_e), \tag{5}$$

where n_c is given by Eq. (3). As n_e gets closer to the critical density, lower power is required to reach relativistic self-focusing. The beam collapse is avoided by the diffraction limit, and these two effects can balance in a dephasing length where acceleration occurs, L_d, in which the wakefield and the electron velocity evolve to be finally in opposite phase. L_d depends on the density through λ_P by:

$$L_d = \lambda_P^3/2\lambda^2. \tag{6}$$

The kinetic energy gained by the electron in the field E_l in the LWFA is given by:

$$\Delta E = e \times E_l \times L_d, \tag{7}$$

and, for λ=0.8 μm:

$$E_l = 0.96\,[n_e\,(\text{cm}^{-3})]^{1/2} \tag{8}$$

The total energy gain given by Eq. (7) results in an energy dependence on the inverse plasma density ($1/n_e$). Increasing the density in the resonant regime results in electron energy in the range of several tens of MeV, many orders magnitude lower than the regular bubble regime with peak powers above 100 TW up to several PW.

A much more flexible alternative regime is the SM-LWFA, which uses a pulse longer than the period of the plasma wave ($c\,\Delta t > \lambda_p$). Therefore, in the length of the optical pulse many plasma wavelengths can be included, modulating the pulse. If the laser peak power corresponds to the

magnitude of the plasma field, allowing the appearance of a zero net transverse electric field, the pulse becomes totally fragmented. This temporal contraction of the fragments along with the decreasing radius of the beam due to self-focusing, given by Eq. (5), can lead the system to a condition of a λ^3 like regime. This highly nonlinear situation leads to a sufficient electron injection in the wakefield when the power exceeds the critical value given by Eq. (5).

We have studied SM-LWFA regime by PIC (Particle-in-Cell) simulations [33] [34] and demonstrated the possibility of producing several tens of MeV electrons in thin, high density gas targets. This is due to a balance between the self-focusing dependence on the density and diffraction, in the length given by Eq. (6). The generation of quasimonoenergetic electron bunches from SM-LWFA is a phenomenon not yet fully understood, despite being demonstrated since 2006 [32, 35]. We have observed that there is a critical dependence on the plasma density and the electron bursts were observed only in a fraction of the laser shots and this has been recently demonstrated by many groups [36-38]. The simulation study of the SM-LWFA is described below.

III. PIC SIMULATIONS

We have been performing PIC simulations [34] to determine the threshold conditions for electrons acceleration in TW level laser systems. These simulations allow observing the interaction between the pulses and the plasma under a wide range of energy conditions, time duration, gas, electron density, focusing, etc., which would be difficult to implement experimentally.

Fig. 1 shows results of a PIC simulation of a 50 fs and 2 TW pulse propagating through a hydrogen gas with an atomic density of 1×10^{20} cm^{-3}. The density map on the top shows the formation of ionic "bubbles", with positive charge density, and the accumulation of negative density (electrons) in well-defined regions. Besides, the laser beam diameter is much smaller (≅ 4 μm) than the original vacuum focused radius of 7 μm, approaching the diffraction limit. In the bottom graphs, the charge density on the axis (blue) clearly shows the accumulation of electrons in bunches, generating a longitudinal electric field distribution, clearly observed in the red graph, which almost reaches 1 TV/m. The periodicity of the charge distribution is in the same order of the diameter of the bubble (also ≅4 μm). These fields are responsible for acceleration of the electrons, that are injected at points where the negative field amplitude is high enough to induce wake breaking. These injected electrons are then accelerated to several MeV. Our simulations have shown that the studied SM-LWFA regime also produces, under certain conditions, monoenergetic electron bunches with low divergence. In our simulations, bunches with mean energy above 10 MeV were produced. The laser requirements for this regime are much simpler than for the few cycle pulses, and pulses as long as 50 fs can be used in the TW and sub-TW regimes. These results correspond to almost the same energy, spread, and charge per bunch as obtained in the λ^3 regimes but with much longer pulses.

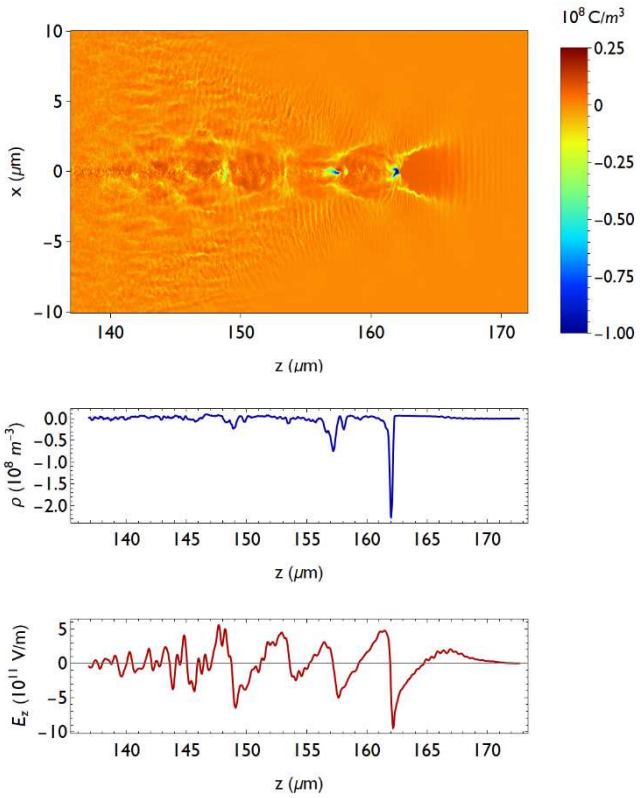

Fig. 1. PIC simulation results for a 2 TW pulse propagatind through H_2 with atomic density of 1×10^{20} cm^{-3}. The top graph shows the charge density (ρ) in the laser polarization plane, and the bottom graphs present the density (blue) and electric field (red) distributions on the pulse propagation axis.

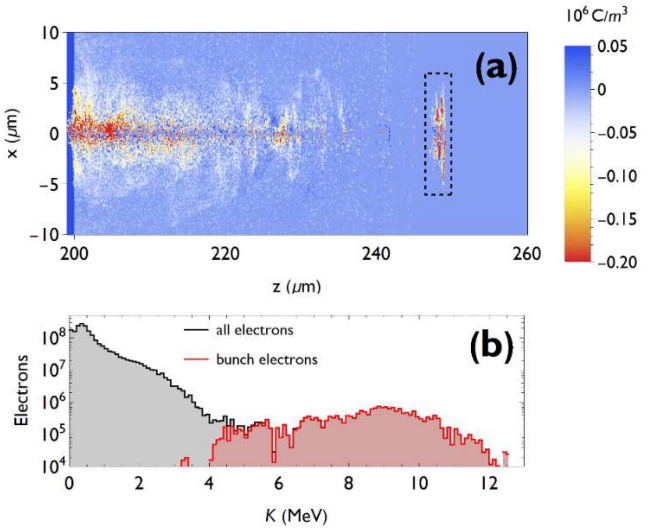

Fig. 2. Results for the simulation with ½ TW and 2×10^{20} cm^{-3}. (a) charge density after ejection from the target evidencing a detached forward bunch (highlighted in a rectangle). (b) Energy spectrum of all ejected electrons (black) and of the bunch (red), with a smooth and broad (9 MeV) peak.

IV. SELECTED CONFIGURATIONS THAT PROVIDE THE MANUFACTURING OF SUB MILLIMETRIC DE LAVAL NOZZLES

Home-made de Laval nozzles were manufactured in an ultrashort pulses micromachining system by trepanning in alumina. The gas jet characterization is made by optical methods, starting with schlieren imaging that localizes the jet, and the gas density is measured by interferometric methods (an in-house developed Mach-Zehnder interferometer). The plasma is characterized by a time-resolved interferometric

diagnostic setup [39]. These two features are also presented at this conference.

V. X-RAY GENERATION BY BREMSSTRAHLUNG, THEIR DEPENDENCE ON ELECTRON KINETIC ENERGY AND THE INDUCTION OF NUCLEAR REACTIONS

Electron beams can be used in medical applications [40-42] either directly, irradiating biological tissues or striking a high-Z material, usually Ta or W, to generate γ and X rays. In the latter case, γ rays can be used to induce photonuclear reactions, leading to the transmutation to radioisotopes of medical interest [43, 44], which is our goal here. Fig. 3 shows the spectral density of the bremsstrahlung radiation generated by impinging a monoenergetic electron beam on a standard Ta thick foil, a conventional technique of γ ray generation in conventional linear accelerators. This mechanism is well known and studies involving conventional accelerators were already done [20] and there are computational codes that allow extracting the emission spectrum. We use the GEANT4 Monte Carlo toolkit [45]. From these spectra, it is possible to see that the electron beam kinetic energy must be greater than tens of MeV to produce large number of photons in the interval between 8 and 20 MeV, which corresponds to an enhancement of photon absorption by most nuclei, known as the Giant Dipole Resonance (GDR). At these energies, after the nuclear excitation, the most probable result is the emission of one neutron.

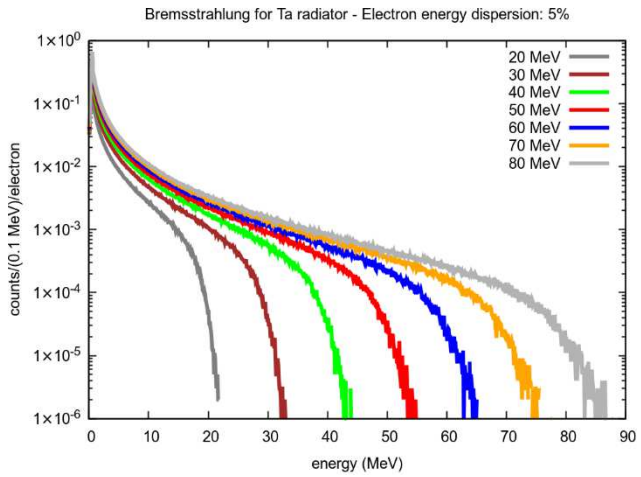

Fig 3. Bremsstrahlung spectra calculated with GEANT4 version 10.6 [45] for electrons impinging on Tantalum target with energies from 20 to 80 MeV with Gaussian dispersion of 5% (sigma).

The goal is to produce ^{99}Mo through the photonuclear reaction ^{100}Mo(γ, n) ^{99m}Mo, which has a γ ray spectral dependence on the reaction cross section [46], as shown in Fig. 4 together with the spectral density of bremsstrahlung photons.

We are defining the optimized electron beam energy to better match the absorption spectrum of the photoneutron reaction and to avoid producing large amounts of other isotopes that can act as contaminants in the sample. Therefore, the optimum energy of the electrons is in the 35 to 40 MeV range, for the defined laser power range of interest here. The mean bremsstrahlung photon efficiency comprising the absorption spectrum of the photoneutron reaction is 0.4 γ ray/electron for the electron kinetic energy of 40 MeV and a Ta foil thickness of 4.4 mm.

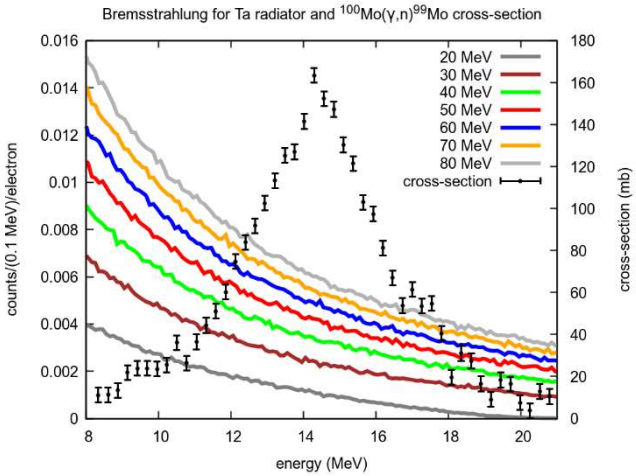

Fig. 4. Absorption cross section for photoproducition of ^{99}Mo in the Giant Dipole Resonance. The right vertical scale corresponds to the absorption cross-section in mb (1 b=10^{-24} cm^2) [46]. The colored lines are the bremsstrahlung spectral density, in the the enrgy interval of the absorption spectrum, for different electron kinetic energies.

VI. TARGET CONSIDERATIONS AND BEAM CHARGE.

In this conceptual design, the SM-LWFA electrons hit a 4.4 mm thick Ta foil. This thickness was optimized by computer simulations (GEANT4) to produce the maximum γ-rays in the absorption band of the photonuclear reaction for 40 MeV electrons. The 100% enriched ^{100}Mo (natural abundance ~10%) is considered isotopically pure due to the possibility of exciting other photonuclear reactions with the other natural isotopes ^{92}Mo, ^{94}Mo, ^{95}Mo, ^{96}Mo, ^{97}Mo and ^{98}Mo. The thickness of the Mo target is 10 mm, with an area of 10 × 10 mm^2. This type of target requires recuperation of the ^{100}Mo after the radiation exposition and therefore the target type and the extraction of the parent nuclei or the desired radioisotope ^{99m}Tc must be revised. As a proof of principle, the gamma decay of the ^{99m}Tc (141 keV) due to the decay time and the desired population will be used as a tracer of the reaction [15]. We stablished an irradiation time of 4 days, longer than the decay time of the ^{100}Mo (66 hours) and the estimated consumption per patient of 370 MBq. A factor 2 must be considered for the US standards (740 MBq) [47]. This 370 MBq activity is equivalent to an initial mass of 20 ng of ^{99}Mo. Due to this small quantity/patient and the long decay of the parent nuclei ^{99}Mo, less efficient methods can be used to produce the radiopharmaceuticals. Using the calculated charge/pulse and the prediction of a laser repetition rate of 1 kHz, the 4 days production will be only 1/26 of the need of a single patient. Taking the assumption that the production of a single clinic is to attend 8 patients per day, the present status of this supposition is a production of only 1/845 for the breakeven in the patient care capacity. Every other concern scales up with this number.

VII. DISCUSSIONS

As pointed out in the previous section, the estimated production capacity of ^{99}Mo must be greatly improved to achieve a chance of success. The first consideration is on the mechanism of electron acceleration. The SM- LWFA regime presents characteristics that can be enhanced. Firstly, it requires long pulses, and usually the pulse energy scale with the pulse duration in the amplification process. Secondly, the manipulation of noticeably short pulses requires special optics, with tight control of the spectral dispersion, including

the target area when the optical beam impinges in the gas jet. Long pulse fluctuations affect the interaction less than in few cycle pulses that are required in λ^3 regime. Besides, the establishment of the SM-LFWA is not so dependent on the pulse duration. We have not examined the dependence of the SM-LWFA regime on this parameter, but as the process is strongly dependent on the nonlinear properties of the plasma near the critical density, we expect a more flexible laser parameters dependence once the criterium of the critical power given by Eq. (5) is obeyed. The SM-LWFA regime is a nonlinear regime and the laws governing the electron beam energy and charge are well known in the literature [32]. They were used to for the PW level power and the GeV energies ranges, and they can be rewritten as:

$$\Delta E\ (\mathrm{MeV}) = 170\ \mathrm{MeV}\ [P(\mathrm{TW})]^{1/3}\, n_e^{-2/3}, \qquad (10)$$

with n_e measured in units of 10^{20} cm^{-3} and

$$q = 2.5\times10^{8}\, P(\mathrm{TW})^{1/2}\ \text{electrons}, \qquad (11)$$

applying for 0.8 μm laser wavelength, P(TW) is the laser peak power in units of TW.

For the simulated case of a 1 TW peak power and a density of 1.6×10^{20} cm^{-3}, the predicted values by Eqs. (10) and (11) are 12 MeV for the energy, and 64 pC for the injected charge, and the simulation calculated values are 12 MeV and 12 pC. Therefore, the value calculated for the energy is close to the theoretical prediction for SM-LFWA regime, but the charge is much below the expected. The scale law for the energy is not strongly dependent on the peak power ($P(\mathrm{TW})^{1/3}$) and it is more dependent on the density ($n_e^{-2/3}$). In the other hand, the theoretical prediction for the charge is not as good as the energy prediction and brings no dependence on the n_e and a smooth dependence on P(TW). This implies that we should search for slightly high-power systems searching for lower plasma densities. For higher charge bunches one possibility is to add a small fraction of N_2 gas that can be up to 5 times ionized at the self-focused spot that achieves relativistic intensities, providing a higher charge injection in the wake. A second alternative is to analyze the injection mechanism in the down ramp, which nowadays can be experimentally tested by the refined process of making the jet nozzles.

VIII. Conclusion

We studied the SM-LWFA regime in the TW peak power region aiming to produce electron beams with energies that could trigger photonuclear reactions capable of producing ^{99}Mo. The optimized electrons kinetic energy for generating γ-rays to produce the parent nucleus ^{99}Mo would be in the 35-40 MeV range. In the current simulation results the yield is half than we have calculated, requiring an improvement of a factor of ~1,700 in the total yield.

Besides, the estimated charge in the bunch that was achieved in the simulations is quite low for SM-LFWA. An initial calculation by simulations was carried to verify if the amount of Mo/Tc produced was significative in the time scale of the radioisotopes decay time (66 h and 6 h, respectively). Using current repetition rate laser technology, the activity produced was very low, ~1/1000 of the required target amount to attend 8 patients per day.

Finally, the overall production efficiency η depends on the average power, that in this case is proportional to the product of the charge/bunch, q, the laser repetition rate f, and the number of producing systems, N, given by $\eta \propto q \times f \times N$. By using the current state of the art TW laser systems, with repetition rates up to a few kHz, the prediction is that the production of the necessary activity amount per patient must increase by 3 orders of magnitude. Just by changing the logistic of supplying ^{99}Mo 6 days after production (t_0+6) there is a gain of a factor 5. Therefore, the repetition rate and charge product must increase by two orders of magnitude to achieve the desired goal. One possible way to reach this goal is by using optical fibers lasers, which are already capable of generating more than 12 kW of average power in pulses with 254 fs [48] at 80 MHz, what would increase the efficiency by a factor 8×10^4. At present, this system pulse energy is ~0.1 mJ, so the peak power does not satisfy the regime simulated in the SM-LWFA yet. Also, short pulses can also be generated in optical fibers using nonlinear effects in thin films and chirped mirrors, producing single cycle optical pulses at 10 MHz [11]. Therefore, the path for operation in high repletion rates and satisfying Eq. (12) is on the way. Also, fiber lasers with an incredible hundred kW high average power are already commercially available [49]. Therefore, a combination of these two results high average power and capability of generating short pulses in high repetition rate, would satisfy the efficiency requirements. As the technology is in the early ages, and medical use is a large-scale market, the future of this application is becoming feasible, despite the necessity of demonstrating and surpassing many challenges.

The demand on nuclear medicine is a growing field, due to the increase in the longevity of the human being and the predominance of coronary diseases and cancer. In both cases, nuclear imaging is a powerful technique that allows physicians to observe the inner organs noninvasively [41]. These techniques are based on high energy radiation, like γ or X rays. So, radiopharmaceuticals are and will be fundamental for the viability of these techniques.

Acknowledgements

The authors acknowledge the support of the funding agencies, FAPESP grant #2018/25961, and CNPq and CAPES for scholarships and research grants. The authors also acknowledge the LNCC - Santos Dumont for providing computational resources for the simulations.

References

[1] T. Tajima, and J. M. Dawson, "Laser Electron Accelerator," Phys. Rev. Lett., vol. 43, pp. 267-270, 1979.

[2] G. Mourou, "Science and applications of the coherent amplifying network (CAN) laser," Eur. Phys. J. Spec. Top., vol. 224, pp. 2527-2528, 2015.

[3] N. D. Powers, "Quasi-monoenergetic and tunable X-rays from a laser-driven Compton light source," Nat. Photonics, vol. 8, pp. 28-31, 2013.

[4] J. P. Palastro, "Dephasingless Laser Wakefield Acceleration," Phys. Rev. Lett., vol. 124, p. 134802, 2020.

[5] D. Strickland, and G. Mourou, "Compression of amplified chirped optical pulses," Opt. Commun., vol. 56, pp. 219-221, 1985.

[6] G. P. Agrawal, and N. A. Olsson, "Self-phase modulation and spectral broadening of optical pulses in semiconductor laser amplifiers," IEEE J. Quantum Elec., vol. 25, pp. 2297-2306, 1989.

[7] M. Nisoli, "Compression of high-energy laser pulses below 5 fs," Opt. Lett., vol. 22, p. 522, 1997.

[8] T. Tajima, and G. Mourou, "Zettawatt-exawatt lasers and their applications in ultrastrong-field physics," Phys. Rev. ST Accel. Beams, vol. 5, 2002.

[9] C. N. Danson, "Petawatt and exawatt class lasers worldwide," High P. Las. Sci. Eng., vol. 7, 2019.

[10] W. P. Leemans, "Experiments and simulations of tunnel-ionized plasmas," Phys. Rev. A, vol. 46, pp. 1091-1105, 1992.

[11] D. Schade, "Single-Cycle Pulse Compression at 10 MHz Repetition Rate in Gas-Filled Hollow-Core Photonic Crystal Fiber," presented at the High Intensity Lasers and High Field Phenomena, 2020.

[12] C. Jauregui, J. Limpert, and A. Tünnermann, "High-power fibre lasers," Nat. Photonics, vol. 7, pp. 861-867, 2013.

[13] R. Polanek, "1 kHz laser accelerated electron beam feasible for radiotherapy uses: A PIC–Monte Carlo based study," Nucl. Instrum. Meth. A, vol. 987, 2021.

[14] H. Lee, "A simulation for the optimization of bremsstrahlung radiation for nuclear applications using laser accelerated electron beam," presented at the FEL2010, Malmö, Sweden, 2010.

[15] Z. Sun, "Review: Production of nuclear medicine radioisotopes with ultra-intense lasers," AIP Advances, vol. 11, 2021.

[16] https://www.energy.gov/nnsa/nnsa-s-molybdenum-99-program-establishing-reliable-supply-mo-99-produced-without-highly, accessed Dec. 2020,

[17] S. Varney, "Inside the Global Relay Race to Deliver Moly-99," in The New York Times, Jan. 12, 2018.

[18] R. G. Bennett, J. D. Christian, D. A. Petti, W. K. Terry, and S. B. Grover, "A System of ^{99m}Tc Production Based on Distributed Electron Accelerators and Thermal Separation," Nuclear Technology, vol. 126, pp. 102-121, 2017.

[19] A. V. Sabel'nikov, O. D. Maslov, L. G. Molokanova, M. V. Gustova, and S. N. Dmitriev, "Preparation of ^{99}Mo and ^{99m}Tc by ^{100}Mo(γ,n) photonuclear reaction on an electron accelerator, MT-25 microtron," Radiochemistry, vol. 48, pp. 191-194, 2006.

[20] H. Naik, S. V. Suryanarayana, A. Gopalakrishna, G. N. Kim, and R. C. Noy, "Production of ^{99}Mo-^{99m}Tc medical isotopes using accelerator as an alternative route," BARC Newsletter, pp. 11-23, 2016.

[21] A. J. Koning, "TENDL: Complete Nuclear Data Library for Innovative Nuclear Science and Technology," Nucl. Data Sheets, vol. 155, pp. 1-55, 2019.

[22] P. Crowther, and J. S. Eldridge, "Decay of 99Mo-99mTc," Nucl. Phys., vol. 66, pp. 472-480, 1965.

[23] P. Verbeek: 'Report on Molybdenum 99 Production for Nuclear Medicine – 2010 – 2020', Association of Imaging Producers & Equipment Suppliers, 2008.

[24] B. M. Dantas, A. L. A. Dantas, F. L. N. Marques, L. Bertelli, and M. G. Stabin, "Determination of ^{99}Mo contamination in a nuclear medicine patient submitted to a diagnostic procedure with ^{99m}Tc," Braz. Arch. Biol. Tech., vol. 48, pp. 215-220, 2005.

[25] J. Faure, "A laser-plasma accelerator producing monoenergetic electron beams," Nature, vol. 431, pp. 541-544, 2004.

[26] C. G. Geddes, "High-quality electron beams from a laser wakefield accelerator using plasma-channel guiding," Nature, vol. 431, pp. 538-541, 2004.

[27] S. P. Mangles, "Monoenergetic beams of relativistic electrons from intense laser-plasma interactions," Nature, vol. 431, pp. 535-538, 2004.

[28] E. Esarey, C. B. Schroeder, and W. P. Leemans, "Physics of laser-driven plasma-based electron accelerators," Rev. Mod. Phys., vol. 81, pp. 1229-1285, 2009.

[29] J. Faure, "A review of recent progress on laser-plasma acceleration at kHz repetition rate," Plasma Phys. Contr. Fus., vol. 61, p. 014012, 2019.

[30] F. Salehi, M. Le, L. Railing, and H. M. Milchberg: 'Laser-accelerated, low divergence 15 MeV quasi-monoenergetic electron bunches at 1 kHz', in arXiv:2010.15720, 2020.

[31] T. Tajima, K. Nakajima, and G. Mourou, "Laser acceleration," Riv. Nuovo Cimento, vol. 40, pp. 33-U102, 2017.

[32] W. Lu, "Generating multi-GeV electron bunches using single stage laser wakefield acceleration in a 3D nonlinear regime," Phys. Rev. ST Accel. Beams, vol. 10, 2007.

[33] R. Lehe, M. Kirchen, I. A. Andriyash, B. B. Godfrey, and J.-L. Vay, "A spectral, quasi-cylindrical and dispersion-free Particle-In-Cell algorithm," Comput. Phys. Commun., vol. 203, pp. 66-82, 2016.

[34] E. P. Maldonado, R. E. Samad, A. V. F. Zuffi, F. B. D. Tabacow, and N. D. V. Junior, "Self-modulated laser-plasma acceleration in a H_2 gas target, simulated in a spectral particle-in-cell algorithm: wakefield and electron bunch properties," in 2019 SBFoton International Optics and Photonics Conference (SBFoton IOPC), 2019.

[35] S. Gordienko, and A. Pukhov, "Scalings for ultrarelativistic laser plasmas and quasimonoenergetic electrons," Phys. Plasmas, vol. 12, 2005.

[36] A. J. Goers, "Multi-MeV Electron Acceleration by Subterawatt Laser Pulses," Phys. Rev. Lett., vol. 115, p. 194802, 2015.

[37] F. Salehi, "MeV electron acceleration at 1 kHz with <10 mJ laser pulses," Opt. Lett., vol. 42, pp. 215-218, 2017.

[38] D. Woodbury, "Laser wakefield acceleration with mid-IR laser pulses," Opt. Lett., vol. 43, pp. 1131-1134, 2018.

[39] A. V. F. Zuffi, E. P. Maldonado, N. D. V. Junior, and R. E. Samad, "Development of a modified Mach-Zehnder interferometer for time and space density measurements for laser wakefield acceleration," in 2021 SBFoton International Optics and Photonics Conference (SBFoton IOPC), in press.

[40] B. S. Nicks, T. Tajima, D. Roa, A. Nečas, and G. Mourou, "Laser-wakefield application to oncology," Int. J. Mod. Phys. A, vol. 34, 2020.

[41] A. Giulietti, Laser-Driven Particle Acceleration Towards Radiobiology and Medicine: Springer International Publishing, 2016.

[42] L. Labate, "Toward an effective use of laser-driven very high energy electrons for radiotherapy: Feasibility assessment of multi-field and intensity modulation irradiation schemes," Sci. Rep., vol. 10, 2020.

[43] J. Jang, "Photonuclear production of self-targeting medical radionuclides using an x-band electron linear accelerator: a feasibility study," in 14th Annual Meeting of Particle Accelerator Society of Japan, 2017.

[44] W. Luo, "No 3 production of radioisotopes of medical interest by photonuclear reaction using eli np γ-ray beam," 2016.

[45] S. Agostinelli, "Geant4—a simulation toolkit," Nucl. Instrum. Meth. A, vol. 506, pp. 250-303, 2003.

[46] M. N. Harakeh, and A. v. d. Woude, Giant resonances : fundamental high-frequency modes of nuclear excitation. Oxford ; New York: Oxford University Press, 2001.

[47] V. Drozdovitch, "Use of Radiopharmaceuticals in Diagnostic Nuclear Medicine in the United States: 1960–2010," Health Phys., vol. 108, pp. 520-537, 2015.

[48] M. Muller, "10.4 kW coherently combined ultrafast fiber laser," Opt. Lett., vol. 45, pp. 3083-3086, 2020.

[49] E. A. Shcherbakov, "Industrial grade 100 kW power CW fiber laser," in *Advanced Solid-State Lasers Congress*, Paris, 2013, p. ATh4A.2.